Journal of Biomechanics 51 (2017) 77–82

Contents lists available at ScienceDirect

Journal of Biomechanics

journal homepage: www.elsevier.com/locate/jbiomech
www.JBiomech.com

In-air versus underwater comparison of 3D reconstruction accuracy using action sport cameras

Gustavo R.D. Bernardina [a], Pietro Cerveri [b], Ricardo M.L. Barros [c], João C.B. Marins [a], Amanda P. Silvatti [a,*]

[a] Department of Physical Education, Universidade Federal de Viçosa, Minas Gerais, Brasil
[b] Department of Electronics, Information and Bioengineering, Politecnico di Milano, Milan, Itália
[c] Faculty of Physical Education, Universidade Estadual de Campinas, São Paulo, Brasil

ARTICLE INFO

Article history:
Accepted 29 November 2016

Keywords:
Camera calibration
3D reconstruction
Action sport cameras
Underwater 3D measurements

ABSTRACT

Action sport cameras (ASC) have achieved a large consensus for recreational purposes due to ongoing cost decrease, image resolution and frame rate increase, along with plug-and-play usability. Consequently, they have been recently considered for sport gesture studies and quantitative athletic performance evaluation. In this paper, we evaluated the potential of two ASCs (GoPro Hero3+) for in-air (laboratory) and underwater (swimming pool) three-dimensional (3D) motion analysis as a function of different camera setups involving the acquisition frequency, image resolution and field of view. This is motivated by the fact that in swimming, movement cycles are characterized by underwater and in-air phases what imposes the technical challenge of having a split volume configuration: an underwater measurement volume observed by underwater cameras and an in-air measurement volume observed by in-air cameras. The reconstruction of whole swimming cycles requires thus merging of simultaneous measurements acquired in both volumes. Characterizing and optimizing the instrumental errors of such a configuration makes mandatory the assessment of the instrumental errors of both volumes.

In order to calibrate the camera stereo pair, black spherical markers placed on two calibration tools, used both in-air and underwater, and a two-step nonlinear optimization were exploited. The 3D reconstruction accuracy of testing markers and the repeatability of the estimated camera parameters accounted for system performance. For both environments, statistical tests were focused on the comparison of the different camera configurations. Then, each camera configuration was compared across the two environments. In all assessed resolutions, and in both environments, the reconstruction error (true distance between the two testing markers) was less than 3mm and the error related to the working volume diagonal was in the range of 1:2000 ($3 \times 1.3 \times 1.5$ m^3) to 1:7000 ($4.5 \times 2.2 \times 1.5$ m^3) in agreement with the literature. Statistically, the 3D accuracy obtained in the in-air environment was poorer ($p < 10^{-5}$) than the one in the underwater environment, across all the tested camera configurations. Related to the repeatability of the camera parameters, we found a very low variability in both environments (1.7% and 2.9%, in-air and underwater). This result encourage the use of ASC technology to perform quantitative reconstruction both in-air and underwater environments.

1. Introduction

Commercial optoelectronic motion capture systems (MOCAPs) have been extensively used to compute the kinematics of many different types of human, animal and robot movements in controlled environments (Chiari et al., 2005; Windolf et al., 2008; Monnet et al., 2014; Safayi et al., 2015), providing results with high three-dimensional (3D) accuracy,[1] ranging from 1:5000 with four cameras (Shortis and Harvey, 1998) to 1:15000 (with respect to the volume diagonal) with 36 cameras (Schmid 2001). Likewise, consumer, industrial and action sport cameras (ASC) have been analyzed as a potential alternative to such systems to obtain reliable outdoor measurements with special interest for uncontrolled and critical environments such as underwater, snow and soccer fields.

* Correspondence to: Departamento de Educação Física, Avenida P. H. Rolfs, s/n°, Campus Universitário. Fax: +55 31 38992249.
E-mail address: amanda.silvatti@gmail.com (A.P. Silvatti).

[1] With the term "accuracy" here we mean the joint of the average and standard deviation errors of a distribution of distances between two points, distributed in the working volume.

http://dx.doi.org/10.1016/j.jbiomech.2016.11.068
0021-9290/

As far as two-dimensional (2D) measurements are concerned, automatic image analysis allowed quantifying the motion of soccer players during games (Barros et al., 2007). As far as three-dimensional (3D) measurements are concerned, it was shown the feasibility of reconstructing ski actions (Baroni et al., 1998) and swimming tasks (Silvatti et al., 2012; Silvatti et al., 2013; Jesus et al., 2015; Bernardina et al., 2016). In particular, ASC technologies, achieving a large consensus for recreational purposes due to ongoing cost decrease, image resolution and frame rate increase, along with plug-and-play usability, have been definitely considered for sport gesture studies and quantitative athletic performance evaluation (Timmis et al.; 2014; Vieira et al., 2015). It is still unclear however whether the setup techniques (scene illumination, image acquisition, image processing, feature tracking, camera calibration objects and methodologies for the estimation of exterior and interior camera parameters), adopted by the commercial optoelectronic systems, can be easily scaled to ASC. For example, the use of active IR and UV illumination sources in outdoor environments is not straightforward, especially underwater, requiring ultra-powerful strobes and custom-engineered band-pass filters (Qualysis, 2015; Optitrack, 2016). In the light of these considerations, the objective of testing the ASC feasibility to quantitative motion analysis is two-fold, namely the focus on the management of measurement errors in terms of camera settings (field of view, image resolution, frame rate) and the arrangement of portable setup techniques. Specifically, in this paper, we evaluate the 3D reconstruction accuracy of two ASCs in-air and underwater. This is motivated by the fact that in swimming, movement cycles are characterized by underwater and in-air phases what imposes the technical challenge of having a split volume configuration: an underwater measurement volume observed by underwater cameras and an in-air measurement volume observed by in-air cameras. Reconstruction of whole swimming cycles would require merging of simultaneous measurements acquired in both volumes. Characterizing and optimizing the instrumental errors of such a configuration requires assessing and synthetizing the instrumental errors of both volumes.

2. Material and methods

2.1. GoPro Hero3+ camera

The Hero3+ camera (GoPro, Black Edition®, 2013 - USA) was considered in this work. Many different camera configurations, provided by the manufacturer, could be chosen by manual setting. First, three fields of view (FOV), namely narrow, medium and wide, were available corresponding to 90, 127, 170° aperture degrees, respectively. For each FOV, a number of possible image resolution and acquisition frequency combinations was available (Table 1). In order to start and stop the camera, we adopted the Wi-Fi remote GoPro control. GoPro studio software was used to convert the acquired videos to AVI movie format. Image processing was based on a custom software tool, named "Dvideo", which was developed and validated by the same authors of the present paper (Figueroa et al., 2003). The marker centroid computation was based on robust morphological operators.

2.2. Stereo-camera attitude and positioning

In order to enable 3D reconstruction, two GoPro Hero3+ cameras were adopted. The camera synchronization was ensured using a flash light in the scene, which identified the initial acquisition frame. The inter-camera and the camera-to-volume distances were set to approximately to 2 and 3.6 m, respectively (Fig. 1). Each camera, mounted on a tripod, was located at a height of about 1 m upon the floor. The same camera positioning was applied in the two different environments, namely in-air and underwater. Considering the three different camera FOVs (narrow, medium and wide) and the stereo-pair positioning, three different acquisition volumes, specifically $3 \times 1.3 \times 1.5$ m^3 (Volume 1), $4 \times 1.8 \times 1.5$ m^3 (Volume 2) and $4.5 \times 2.2 \times 1.5$ m^3 (Volume 3), were obtained (Fig. 1).

Table 1
Camera configurations used to assess the accuracy of the action sport cameras.

Configuration	FOV	Acquistion frequency	Image resolution	Acquistion volume
1	Narrow	120 Hz	1280 × 720p	$3 \times 1.3 \times 1.5$ m^3
2	Narrow	60 Hz	1920 × 1080p	$3 \times 1.3 \times 1.5$ m^3
3	Medium	60 Hz	1280 × 720p	$4 \times 1.8 \times 1.5$ m^3
4	Medium	60 Hz	1920 × 1080p	$4 \times 1.8 \times 1.5$ m^3
5	Wide	240 Hz	848 × 480p	$4.5 \times 2.2 \times 1.5$ m^3
6	Wide	120 Hz	1280 × 720p	$4.5 \times 2.2 \times 1.5$ m^3
7	Wide	100 Hz	1280 × 960p	$4.5 \times 2.2 \times 1.5$ m^3
8	Wide	60 Hz	1920 × 1080p	$4.5 \times 2.2 \times 1.5$ m^3
9	Wide	48 Hz	1920 × 1440p	$4.5 \times 2.2 \times 1.5$ m^3

2.3. Camera calibration

The camera calibration was carried out to estimate both the interior (focal length, principal point and x/y scale) and the exterior (position and orientation of the camera with respect to the reference coordinate system) parameters of both cameras. A radial/tangential optical distortions were included in the camera perspective model.

The calibration was performed in two steps encompassing the acquisition of one static and one moving object (Fig. 1, calibration tools). The static object consisted in a waterproof orthogonal triad structure ($1 \times 1 \times 1$ m), with nine spherical black markers (⌀: 35 mm) in known positions, with respect to the origin of the triad. The nine markers were used to determine the reference coordinate system (Silvatti et al., 2012). The moving object was a wand, carrying two spherical markers (⌀: 35 mm) at a known distance (d_n: 250 mm) (Bernardina et al., 2016). Both tools were manufactured by computer numerical control.

In the first step, the triad was placed on the floor, in the center of stereo-pair FOV and acquired for 5 s. For each camera, the image points of the markers and the corresponding 3D coordinates of the triad markers were used in the direct linear transform (DLT) algorithm (Hatze, 1998; Abdel-Aziz and Karara, 1971) to estimate both the interior and the exterior parameters disregarding the optical distortions. In the second step, the triad was detached from the scene and the wand was moved, for about 20 s, within the volume as much as to cover the two camera image planes and the two markers were acquired. Out of the total acquired frames, exactly 100 wand positions, homogeneously distributed in the working volume, were used in a bundle adjustment refinement of the camera parameters including optical distortion model. The camera model was supplemented with one single radial parameter k_1 when using the narrow camera FOV, two radial parameters k_1 and k_2 when using the medium FOV and two radial, along with one additional tangential p_1, parameters when using the wide FOV. The calibration algorithm used the initial stereo-pair parameters (estimated by the DLT algorithm) and the 2D coordinates of the 200 wand positions to refine the camera parameters, estimate the distortion parameters and compute the 3D coordinates of the wand markers. The distance between the two markers was exploited as an additional constrain in the bundle. The implementation of the camera calibration was based on a custom development, whose validation was reported in early literature by the same authors of the present paper (Cerveri et al., 1998; Cerveri et al., 2001).

2.4. Performance evaluation

2.4.1. 3D reconstruction accuracy

The 3D reconstruction accuracy of the ASC pair was studied as a function of the camera configuration. A camera configuration was defined as a combination of FOV, acquisition frequency, image resolution and acquisition volume (Table 1). Each configuration was tested both underwater and in-air conditions. The 3D accuracy was analyzed in a rigid bar test (five acquisition trials lasting at least 10 s each), using the same wand adopted in the calibration stage. The wand tool, equipped with the two testing markers, was moved within the working volume to cover as much as possible both the camera image planes. Irrespective of acquisition frequency and FOV, 4000 wand distances, homogeneously distributed within the working volume, were collected from the five trials.

Using the 4000 reconstructed distances, the following errors were considered: a) mean of the distance error distribution (ME) to quantify the bias of the reconstruction; b) the standard deviation of the distance error distribution (SD) to quantify the precision of the reconstruction; c) the mean absolute value of the distance error distribution (MAE) to quantify the overall accuracy of the reconstruction; d) the percentage error (the ratio between the MAE and the maximum diagonal of the working volume) to refer the overall accuracy to the target working volume and making it comparable across different volume sizes (Chiari et al., 2005).

In order to compare the different camera configurations (Table 1) for each environment (in-air/underwater), we adopted the Kruskal–Wallis non-parametric test with Tukey post-hoc comparison ($p=0.05$). In order to compare the same

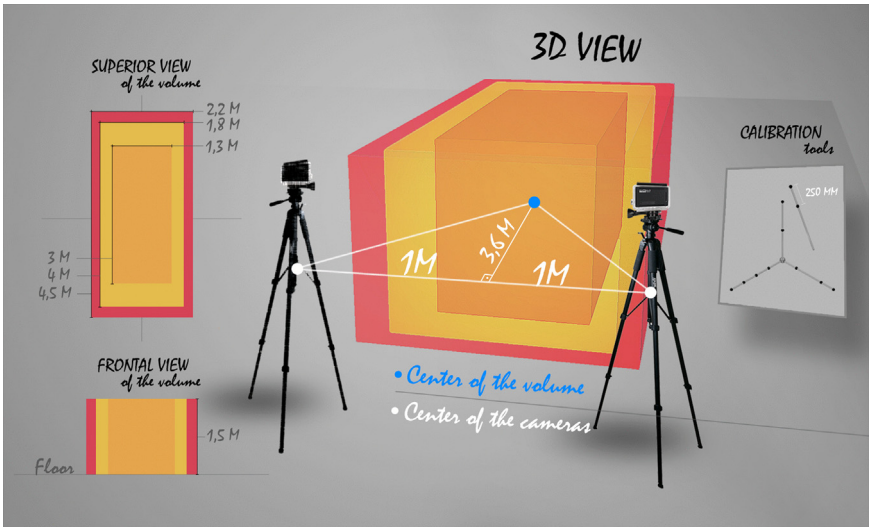

Fig. 1. Stereo-camera positioning along with the three different working volumes corresponding to the three FOVs, 3D, superior and frontal view of the volume. Calibration tools, wand and triad used to calibrate the cameras.

camera setup across the two environments we adopted the Wilcoxon–Mann–Whitney non-parametric test ($p=0.05$). For both statistical tests, the distribution of the 4000 mean absolute distance errors were used. All the analysis was performed in Matlab (release 2015b) software (Matworks Natick, USA).

2.4.2. Repeatability of the camera parameters

In order to assess the repeatability of the camera parameters (interior, exterior and distortion parameters), we chosen the camera configuration providing the highest accuracy results. Ten different acquisitions of calibration wand data were used to estimate ten calibration parameters sets. The repeatability was reported in terms of the variability of each camera parameter about its corresponding average value across the ten calibrations.

3. Results

3.1. 3D reconstruction accuracy

In all assessed resolutions, and in both environments, the MAE was less than 3 mm (Table 2). The best and the worst MAE values were 0.60 mm (1:7000)[2] and 2.76 mm (1:2000), in the configuration 2 and configuration 5, both in the underwater environment, respectively. Interestingly, all the in-air calibrations provided a negative bias of the mean error whereas the underwater calibrations led on average to a positive bias. Further, the SD and the MAE for the in-air values were consistently larger than the one for the underwater tests. No specific dependency of the error on the distribution of the markers in space was appreciated. Provided that the camera positioning was very similar and the camera FOV was exactly equal in each configuration, the error bias discrepancy between in-air and underwater environments could be ascribed to some issues in the marker centroid detection or optical distortion effects. In Fig. 2, we show the camera images of two paradigmatic configurations (config. #2 and config. #8). The different optical distortion effects are clearly visible, with greater fisheye effect in the in-air environment. As a consequence, the estimated distortion parameters were higher in the in-air (config.2, only k_1: camera #1: −0.30; camera #2: −0.28; config.8, k_1, k_2, p_1: camera #1: −0.28, −0.08, 0.004; camera #2: −0.27, −0.09, 0.003) than in underwater (config.2, only k_1: camera #1: −0.05; camera #2: −0.09; config.8, k_1, k_2, p_1: camera #1: −0.19, 0.80, −0.002; camera #2: −0.13, 0.10, −0.009). This discrepancy between the parameter values found can be ascribed reasonably to the change of the medium from air to water.

Table 2
Results of the rigid bar test (4000 samples) in all camera configurations, in both environments. Nominal distance d_n between the two markers: 250 mm.

FOV	Configurations	Environment	ME ± SD [mm]	MAE [mm]
Narrow (90°)	1	Underwater	0.57±0.87	0.82
		In-air	−0.69±0.96	1.03
	2	Underwater	0.08±0.77	0.60
		In-air	−0.67±0.99	0.97
Medium (127°)	3	Underwater	0.20±1.11	0.89
		In-air	−0.47±1.86	1.49
	4	Underwater	0.09±0.77	0.61
		In-air	−0.47±1.13	0.97
Wide (170°)	5	Underwater	−0.39±3.51	2.76
		In-air	−0.77±3.72	2.67
	6	Underwater	0.02±1.88	1.44
		In-air	−0.77±2.04	1.66
	7	Underwater	0.23±2.02	1.62
		In-air	−0.31±2.19	1.66
	8	Underwater	0.37±0.98	0.79
		In-air	−0.60±1.42	1.23
	9	Underwater	0.60±1.11	1.00
		In-air	−0.81±1.53	1.37

In both environments, the comparison between the camera configurations 1 and 2 (same FOV, but different acquisition frequencies and image resolutions) revealed significant lower accuracy results in the configuration 1 ($p < 10^{-5}$). Similarly, when we evaluated only the configurations with the wide FOV (5, 6, 7, 8, and 9), as expected, the configuration with the lower image resolution (5), in both environments, provided the worst accuracy results ($p < 10^{-5}$) (Table 2) Fig. 3.

[2] Reference to the working volume diagonal.

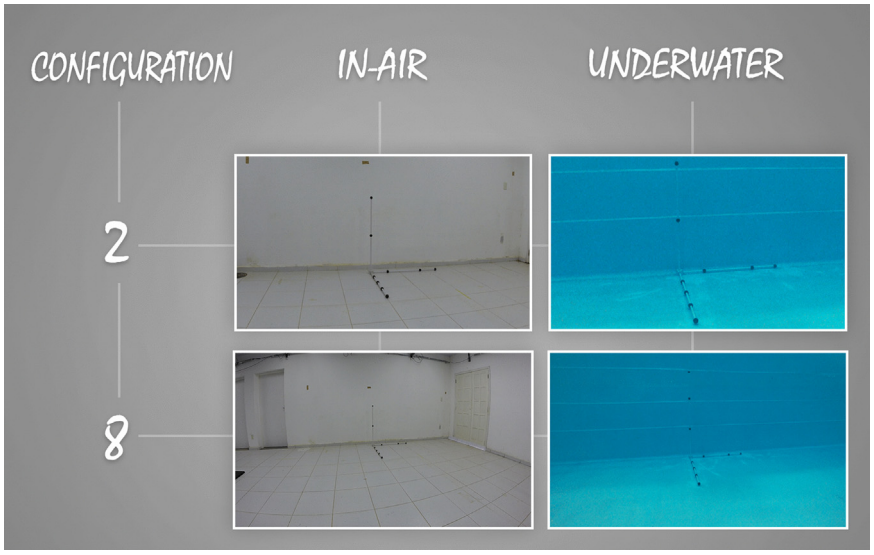

Fig. 2. Images of the triad acquisition to show the different in the optical distortion in-air and in the underwater environment.

In order to evaluate how the FOV affected the 3D accuracy, we compared the configurations 2, 4 and 8, having all the three the same image resolution and frequency. No difference (in-air and underwater: $p=0.99$) in the narrow and medium FOV was found. Conversely, for the wide FOV the MAE was significantly worse than the other two FOVs ($p < 10^{-5}$) both in-air and underwater (Table 2).

In order to evaluate how the image resolution affected the 3D accuracy, we compared the configurations 3 and 4, having both the same FOV and frequency. As expected, in the high image resolution we found errors significantly lower than the one in the low image resolution (in-air and underwater: $p < 10^{-5}$). Statistically, the 3D accuracy obtained in the in-air environment was poorer ($p < 10^{-5}$) than the one in the underwater environment, across all the tested camera configurations.

3.2. Repeatability of the camera parameters

On average, the camera parameter variability was lower than 1.7% and 2.9% for in-air and underwater, respectively (Table 3). The most variable parameter was the γ angle (orientation of the Z axis of the camera coordinate system with respect to the reference coordinate system) for in-air environment and the principal point coordinates for the underwater environment. The computed inter-camera distance was on average 1945.5 (± 4.6) and 2208.5 mm (± 7.0) for the underwater and in-air calibrations, respectively. As far as optical distortions are concerned, the averaged radial parameter k_1 differed sensibly between in-air (camera #1: -0.32 ± 0.01; camera #2: -0.27 ± 0.01) and underwater (camera #1: -0.05 ± 0.01; camera #2: -0.09 ± 0.02) environments, in agreement with the above results.

4. Discussion and conclusions

Aiming at enabling the 3D swimming motion analysis, which is characterized by movement cycles in underwater and in-air phases, the first fundamental step consists of characterizing the 3D reconstruction accuracy in underwater and in-air environments. In this work, we proposed the use of ASCs, alternative to traditional MOCAPs, for swimming quantitative analysis and we evaluated the 3D reconstruction accuracy underwater in comparison to in-air.

For the in-air environment, the MOCAPs applied to gait analysis were extensive evaluated and showed that the reconstruction accuracy can range from 0.5 to 11 mm as a function of the number of cameras in the typical working volume of $6 \times 1.5 \times 2$ m (Chiari et al. 1996; Ehara et al. 1997; Richards 1999; Pribanić et al., 2008; Eichelberger et al., 2016). The evolution of such technologies, including active optical filters, allowed extending the motion capture to outdoor and underwater environments, ensuring sub-millimeter reconstruction accuracy when using a large number of cameras (Vicon, 2016; BTS Bioengineering 2014; Qualysis, 2014; Motion Analysis Corporation, 2016; Optitrack, 2016).

Industrial and ASCs cameras represent a less expensive alternative to MOCAPs for outdoor and underwater environments. Jump, football kick and combat actions are examples of possible outdoor applications that can be analyzed quantitatively adopting such technologies (Payton, 2008). Likewise, water walking and swimming tasks are expected examples of underwater applications (Ceseracciu, et al. 2014; Silvatti et al., 2013; Mooney et al., 2015). Using devoted camera calibration protocols, acceptable accuracy results (0.7–3.0 mm) were reported (Silvatti et al., 2012; Balletti et al., 2014; Shortis 2015; Helmholz, et al. 2016; Bernardina et al., 2016; Jackson et al., 2016). In underwater analysis, two

Table 3
Variability of the calibration parameters in both environments across ten repeated calibrations.

Environment	Cam	Location [%]			Rotation angles [%]			Principal point [%]		Focal length [%]	
		X	Y	Z	α	β	γ	x	y	f/c_x	f/c_y
Underwater	1	0.24	0.23	0.15	0.65	0.13	0.35	1.24	1.28	0.20	0.24
	2	0.24	0.36	0.18	0.59	0.53	1.91	0.85	2.89	0.18	0.27
In-air	1	0.21	0.29	0.25	0.27	0.38	1.61	1.02	0.78	0.20	0.23
	2	0.19	0.37	0.21	0.60	0.21	0.34	0.51	0.99	0.24	0.29

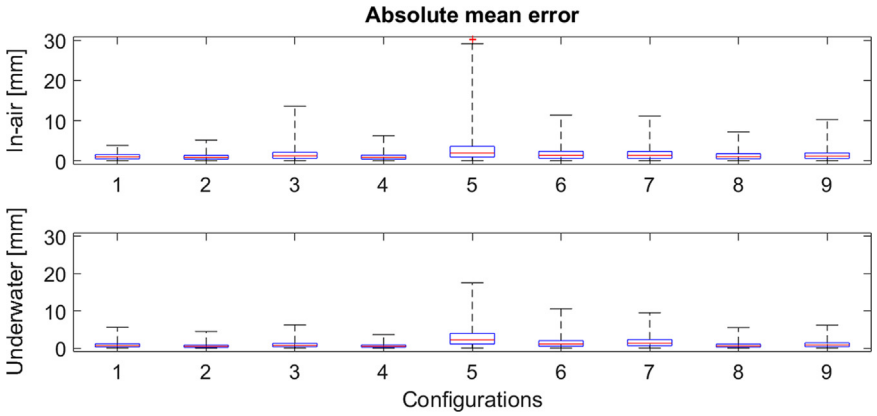

Fig. 3. MAE distribution in the nine camera configurations tested for underwater (upper panel) and in air (laboratory, lower panel) environments.

industrial Basler cameras provided a reconstruction accuracy lower than 1.15 mm (1:4000) (Silvatti et al., 2012). Two ASCs were reported to ensure a reconstruction accuracy underwater of 1.00 mm on average (1:1000) (Shortis, 2015). Again, two ASCs provided a reconstruction accuracy underwater of 1.20 mm on average (1:3000) (Bernardina et al. 2016). In outdoor motion capture, three ASCs were reported to provide a 3D reconstruction accuracy of 7.20 mm (1:10000) (Jackson et al., 2016). In the present paper, our best and worst accuracy results, in both environments, were in nice agreement (Table 2) with such earlier results. As far as geometric camera parameters are concerned, we found a very low variability in both environments since the maximum values (1.7% in-air and 2.9% underwater) were less than 5% in agreement with the literature (Cerveri et al. 1998). As far as the acquisition frequency and the image resolution are concerned, as expected the resolution revealed to be more decisive. The configurations 2 and 4 (1920×1080, 60 Hz) were those that provided the best accuracy (Table 2). Despite of the highest available acquisition frequency (240 Hz), poor results were found when using a low image resolution (848×480 pixel). As expected, the wide FOV affected negatively the accuracy results, supported by the comparison between the config. 1 and 6 and the config. 2 and 8. In both cases, the frequency and image resolution were the same and only the FOV changed (narrow to wide), and the accuracies were worst in the configurations with the wide FOV (config. 6 and 8).

As a general finding, we showed that an ASC pair can be configured to survey an underwater working volume size ranging from 5.85 m^3 to 14.85 m^3, providing the best accuracy of 0.60 and 0.80 mm, respectively. As well, our results support the possibility to use ASCs at high frame rate (240 Hz) suitable to survey fast movements, as running, cycling and kicks (Tables 1 and 2), however tolerating a decrease of accuracy. As a specific finding, we remark that significant higher accuracy results were found in the underwater than in the in-air environment. As above anticipated, this can be explained by the effect of the fish-eye lens and the marker centroid detection. In underwater, we found less effect of the fish-eye lens than in-air (Fig. 2). The camera calibration took this fact into account and estimated higher values of the optical distortion parameters, as reported in the result section. Despite the camera calibration calculated the adjustment of the optical distortion, the MAE values were significantly still different. Additionally, the use of black markers provided a better background-foreground contrast in the underwater images. This ensured a lower error in the 2D marker centroid detection than the detection performed on in-air images. It is relevant to point out however that the image processing algorithms, used to compute the markers centroid, were based on morphologic operators. More robust methods, based on circle fitting, could increase the 2D detection accuracy.

In the light of this synthesis, it is reasonable to assert that ASC is a cost-effective technology to perform quantitative reconstruction both in-air and underwater. In order to analyze a complete 3D swimming cycle is necessary however to integrate both environments addressing the definition of a common coordinate system and the synchronization of the in-air and underwater cameras. In addition, the use of surface markers still remains an issue for the tracking because of water drag that produces bubbles, and markerless analysis seems a natural development to overcome this problem (Ceseracciu et al., 2014). Future works will include also the cross-validation with commercial optoelectronic systems and the evaluation of multiple action sport cameras, even mobile, to increase the working volume size along with proper setup procedures (e.g. calibration, motion tracking).

Conflict of interest

The authors of this paper certify that they have NO affiliations with or involvement in any organization or entity with any financial interest (such as honoraria; educational grants; participation in speakers' bureaus; membership, employment, consultancies, stock ownership, or other equity interest; and expert testimony or patent-licensing arrangements), or non-financial interest (such as personal or professional relationships, affiliations, knowledge or beliefs) in the subject matter or materials discussed in this manuscript.

Acknowledgments

Research supported by FAPESP (00/01293-1, 2006/02403-1 and 2009/09359-6), CNPq (473729/2008-3, 304975/2009-5, 478120/2011-7, 234088/2014-1, and 481391/2013-4), CAPES (2011/10-7 and 08/2014) and FAPEMIG (PEE-00596-14).

References

Abdel-Aziz, Y.I., Karara. H.M. 1971. Direct linear transformation from comparator coordinates into object space coordinates in close-range photogrammetry. In: Proceedings of the Symposium on Close-Range Photogrammetry. American Society of Photogrammetry, Falls Church.

Balletti, C., Guerra, F., Tsioukas, V., Vernier, P., 2014. Calibration of action cameras for photogrammetric purposes. Sensors 14 (9), 17471–17490.

Baroni, G., Ferrigno, G., Rodano, R., 1998. Three-dimensional sport movement analysis by means of free floating tv cameras with variable optics. In: Proceedings of the 16 International Symposium on Biomechanics in Sports, Konstanz, Germany.

Barros, R.M.L., Misuta, M.S., Menezes, R.P., Figueroa, P.J., Moura, F.A., Cunha, S.A., Anido, R., Leite, N.J., 2007. Analysis of the distances covered by first division Brazilian soccer players obtained with an automatic tracking method. J. Sport. Sci. Med. 6, 233–242.

Bernardina, G.R.D., Cerveri, P., Barros, R.M.L., Marins, J.C.B., Silvatti, A.P., 2016. Action sport cameras as an instrument to perform a 3D underwater motion analysis. PLoS ONE 11 (8), 1–14.

BTS Bioengineering, 2014. BTS Smart DX. Avaliable: http://www.btsbioengineering.com/wp-content/uploads/2014/02/BTSBRO_SMART-DX-1113UK_LQ.pdf.

Cerveri, P., Borghese, N.A., Pedotti, A., 1998. Complete calibration of a stereo photogrammetric system through control points of unknown coordinates. J. Biomech. 31 (10), 935–940.

Cerveri, P., Pedotti, A., Borghese, N.A., 2001. Combined evolution strategies for dynamic calibration of video-based measurement systems. IEEE Trans. Evol. Comput. 5 (3), 271–282.

Ceseracciu, E., Sawacha, Z., Cobelli, C., 2014. Comparison of markerless and marker-based motion capture technologies through simultaneous data collection during gait: proof of concept. PLoS One 9 (3), e87640.

Chiari, L., Croce, U.D., Leardini, A., Cappozzo, A., 2005. Human movement analysis using stereophotogrammetry. Part 2: instrumental errors. Gait Posture 21 (2), 197–211.

Ehara, Y., Fujimoto, H., Miyazaki, S., Mochimaru, M., Tanaka, S., Yamamoto, S., 1997. Comparison of the performance of 3D camera systems II. Gait Posture 5 (3), 251–255.

Eichelberger, P., Ferraro, M., Minder, U., Denton, T., Blasimann, A., Krause, F., Baur, H., 2016. Analysis of accuracy in optical motion capture – A protocol for laboratory setup evaluation. J. Biomech. 49, 2085–2088.

Figueroa, P.J., Leite, N.J., Barros, R.M.L., 2003. A flexible software for tracking of markers used in human motion analysis. Comput. Methods Prog. Biomed. 72 (2), 155–165.

Hatze, H. 1998. High-precision three-dimensional photogrammetric calibration and object space reconstruction using a modified DLT-approach. 21(7), pp. 533–538.

Helmholz, P., Long, J., Munsie, T., Belton, D., 2016. Accuracy assessment of Go Pro Hero 3 (black) camera in underwater environment. Int. Arch. Photogramm. Remote Sens. Spat. Inf. Sci. 41, 477–483.

Jackson, B.E., Evangelista, D.J., Ray, D.D., Hedrick, T.L., 2016. 3D for the people: multi-camera motion capture in the field with consumer-grade cameras and open source software. Biol. Open . http://dx.doi.org/10.1242/bio.018713.

Jesus, K., Jesus, K., Figueiredo, P., Vilas-Boas, J.P., Fernandes, R.J., Machado, L.J., 2015. Reconstruction accuracy assessment of surface and underwater 3D motion analysis: a new approach. Comput. Math. Methods Med., 1–8.

Monnet, T., Samson, M., Bernard, A., David, L., Lacouture, P., 2014. Measurement of three-dimensional hand kinematics during swimming with a motion capture system: a feasibility study. Sport. Eng. 17 (3), 171–181.

Mooney, R., Corley, G., Godfrey, A., Osborough, C., Quinlan, L.R., OLaighin, G., 2015. Application of video-based methods for competitive swimming analysis: a systematic review. Sports and Exercise. Sports Excercise Med. 1 (5), 133–150.

Motion Analysis Corporation, 2016. Movement analysis products. Available: ⟨http://www.motionanalysis.com/html/movement/products.html⟩.

Optitrack, 2016. Available: ⟨http://www.optitrack.com/motion-capture-movement-sciences/⟩.

Payton, C.J., 2008. Motion analysis using video. In: Payton, C.J., Barlett, R.M. (Eds.), Biomechanical evaluation of movement in sport and exercise: The British Association of Sport and Exercise Sciences Guidelines. Routledge, London and New York, pp. 8–32.

PribanićT., SturmP., CifrekM., 2008. Calibration of 3D kinematic systems using 2D calibration plate. In: Proceedings of the XXVI International Symposium on Biomechanics in Sports. Seoul, Korea.

Qualysis, O., 2015. Available: ⟨http://www.qualisys.com⟩.

Richards, J., 1999. The measurement of human motion: a comparison of commercially available systems. Human Mov. Sci. 18, 589–602.

Safayi, S., Jeffery, N.D., Shivapour, S.K., Zamanighomi, M., Zylstra, T.J., Bratsch-Prince, J., Wilson, S., Reddy, C.G., Fredericks, D.C., Gillies, G.T., Howard, M.A., 2015. Kinematic analysis of the gait of adult sheep during treadmill locomotion: parameter values, allowable total error, and potential for use in evaluating spinal cord injury. J. Neurol. Sci. 358, 107–112.

Silvatti, A.P., Dias, F.A.S., Cerveri, P., Barros, R.M.L., 2012. Comparison of different camera calibration approaches for underwater applications. J. Biomech. 45 (6), 1112–1116.

Silvatti, A.P., Cerveri, P., Telles, T., Dias, F.A.Z., Baroni, G., Barros, R.M.L., 2013. Quantitative underwater 3D motion analysis using submerged video cameras: accuracy analysis and trajectory reconstruction. Comput. Methods Biomech. Biomed. Eng. 16 (11), 1240–1248.

Shortis, M.R., Harvey, E.S., 1998. Design and calibration of an underwater stereo-video system for the monitoring of marine fauna populations. Int. Arch. Photogramm. Remote Sens. 32, 792–799.

Shortis, M.R., 2015. Calibration techniques for accurate measurements by underwater camera systems. Sensors 15 (12), 30810–30826.

Schmid, O.A., 2001. A new calibration method for 3-D position measurement in biomedical applications. Biomed. Tech. 46, 50–54.

Timmis, M.A., Turner, K., van Paridon, K.N., 2014. Visual search strategies of soccer players executing a power vs. placement penalty kick. PLoS One 9 (12), 115–179.

Vicon. B., 2016. Availible: ⟨https://www.vicon.com/file/vicon/bonita-brochure.pdf⟩.

Vieira, L.H.P., Pagnoca, E.A., Milioni, F., Barbieri, R.A., Menezes, R.P., Alvarez, L., Déniz, L.G., Santana-Cedrés, D., Santiago, P.R.P., 2015. Tracking futsal players with a wide-angle lens camera: accuracy analysis of the radial distortion correction based on an improved Hough transform algorithm. Comput. Methods Biomech. Biomed. Eng. Imaging Vis. 0, 1–11. http://dx.doi.org/10.1080/21681163.2015.1072055.

Windolf, M., Gotzen, N., Morlock, M., 2008. Systematic accuracy and precision analysis of video motion capturing systems – exemplified on the Vicon-460 system. J. Biomech. 41, 2776–2780.